Lasers in Manufacturing Conference 2019

Effects of hot isostatic pressing and solution annealing on microstructure and porosity of tool steel 1.2709 processed by selective laser melting

Johannes Pantring[a], André Edelmann[a*], Ralf Hellmann[a]

[a]*University of Applied Sciences Aschaffenburg, Würzburger Str. 45, 63743 Aschaffenburg, Germany*

Abstract

Selective laser melting (SLM) is a well-known additive manufacturing technique of metallic components. Weldable materials like iron-based alloys or nickel-based alloys can be processed. Due to the laser-based fabrication process, SLM parts are characterized by a fine grain microstructure, anisotropic mechanical properties and porosity in volume. These properties are limiting applications of SLM fabricated components. Thermal post processing of additive manufactured components allows to modify the properties of SLM parts. This can lead to an improvement of the part quality and can thereby open new fields of applications. Here we discuss and compare the thermal post processing steps of solution annealing and hot isostatic pressing to modify the microstructure and the porosity of tool steel 1.2709 SLM-parts. Solution annealing bears to the microstructure of the SLM-part and homogenize the grain structure. Hot isostatic pressing (HIP) enables thermal treatment under gas pressures. The HIP process can reduce internal porosity of the SLM-part which can improve e.g. the scattering and anisotropic characteristic of the mechanical properties. We study the effects of solution annealing and hot isostatic pressing regarding microstructure, porosity and directional mechanical properties.

Keywords: selective laser melting, hot isostatic pressing, mechanical properties;

* Corresponding author. Tel.: +0-000-000-0000 ; fax: +0-000-000-0000 .
E-mail address: author@institute.xxx .

1. Introduction

The additive manufacturing (AM) technology of selective laser melting allows the fabrication of highly complex metallic parts. The layer-wise fabrication process is based on fine-sized metallic powder fused by laser processing. Detail information of the SLM process can be found e.g. in Gibson, 2015; Yap, 2015. The AM-technology allows new degrees of freedom in component fabrication and novel designs become available. Applications can be found in a wide range of industrial sectors, e.g. in aerospace or tool construction Seabra, 2016; Colter, 2017.

Mechanical properties in general depends besides the used material composition on specific characteristics of the manufacturing technology Ilscher, 2010. In the SLM process these characteristics lead to thermal induced residual stresses, fine-grain sized and directional microstructure as well as porosity in the volume Niendorf, 2013; Buchmayer 2013; Kruth 2010. Thermal induced residual stress appears due to high heating and cooling rates by laser processing of the metallic powder. As result large deformation of the part geometry can occur Mercelis, 2006. The fine-grain sized microstructure of SLM parts arise from high cooling rates of the melt pool after laser processing. The predominant direction of the grains are formed according to the direction of the thermal gradients. These effects induce anisotropic mechanical properties and regarding to the Hall-Petch relation higher strength of the SLM part compared e.g. with casted parts Niendorf, 2013; Rösler, 2016; Kemper, 2011. The achievable porosity in the part volume is typically below 1%. However this small amount of the porosity can reduce the part quality e.g. their dynamic load characteristic Cáceres, 1996; Cherry, 2015. Several reason can be identified for the formation of porosity while SLM processing. If the laser power is too high, smaller metallic powder particles vaporize and spherical gas pores in the volume occur Ganeriwala, 2016; Wessels 2017. If the fusion of the processed powder layer to the already fabricated layers is incomplete, the so called lack-of-fusion porosity can appear. These pores are typically longish, perpendicular to the build direction and randomly-shaped Karg, 2012; Wessels, 2017; Khairallah, 2014. The lack-of-fusion porosity has one of the major influences to the mechanical properties. The sharp-edged structure involves focusing of mechanical strains in these edges and as result delamination or cracks can occur that reduce the SLM part quality Zang, 2017; Wycisk, 2017. These specific SLM part characteristics can be improved by thermal post processing. For example the thermal induced residual stresses can be reduced by using stress relief annealing. The microstructure can be modified by solution annealing and by applying hot isostatic pressing, the porosity in the volume can be reduced.

In this article we analyze the thermal treatment of solution annealing and hot isostatic pressing by studying the microstructure and the tensile strength of SLM fabricated specimens. We are focused on maraging tool steel 1.2709 which is widespread in industrial application e.g. for injection molding tools. In particular the material can be machined after the SLM process and is therefore suitable for hybrid additive manufacturing systems that combines SLM and milling Du, 2018.

2. Specimens and thermal treatment

We fabricate tensile test specimens to analyze the influence of heat treatments of SLM parts. The design of the tensile test specimen refers to DIN 50125 type A. The dimension are shown in Fig.1. To study the directional mechanical properties the specimens are fabricated in the orientations of 0°, 22.5°, 45°, 67,5° and 90° to the building platform.

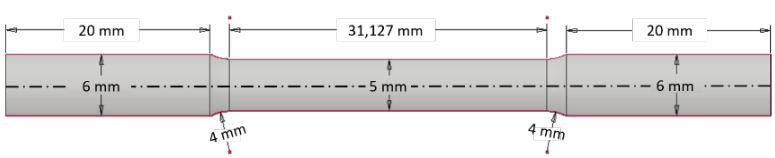

Fig. 1. Dimension of the tensile test specimens based on DIN 50125 type A

For SLM fabrication of the specimens we use the system LaserTec 30, DMG Mori. The SLM process parameters are as follows: layer thickness t_{Layer} = 50 µm, laser power P_l = 160 W, exposure time t_{exp} = 40 µs, point distance d_{point} = 40 µm, hatch distance d_{hatch} = 90 µm and hatch rotation ϕ_{hatch} = 67°. The metallic powder of maraging tool steel 1.2709 is provided by LPW Technology. The particle size distribution of the powder has its median at p_{median} = 26,5 µm. The 10%- and 90%-quantiles are $p_{10\%}$ = 16,1 µm and $p_{90\%}$ = 40,7 µm. The chemical compositions is according Tab.1. As typical for maraging steel a low amount of carbon (C) and the high amount of nickel (Ni) can be found.

Table 1.1. Composition of maraging tool steel 1.2709

	Fe	C	Si	Mn	Cr	Mo	Ni	Co	Ti	Nb	S
1.2709 vol.[%]	balance	<0.03	<0.1	<0.15	<0.25	4.5 – 5.2	17 - 19	8.5-10	0.8-1.2	-	< 0.01

We study the effect of thermal treatments of solution annealing (SA), hot isostatic pressing (HIP) compared to the as-build (AB) condition directly after SLM fabrication. We fabricate 60 tensile test specimens by analyzing four specimens in each build orientation of 0°, 22.5°, 45°, 67,5° and 90° for the process conditions of AB, SA, HIP.

The temperature and pressure profile used for the HIP cycle is shown in Figure 2. The temperature profile (red) starts with heating up to ϑ_{max} = 1100°C using a heating rate of $\Delta\vartheta_{heat}$ = 5 K/min. After holding time of t_{hold} = 2 we cool down by rapid cooling to ϑ_{min} = 20°C with cooling rate of approximately $\Delta\vartheta_{cool}$ = 36 K/s. The pressure profile (blue) is close to the temperature profile with maximum pressure of p_{max} = 1000 bar. These HIP recipe is most commonly used for hot isostatic pressing of steel Atkinson, 2000.

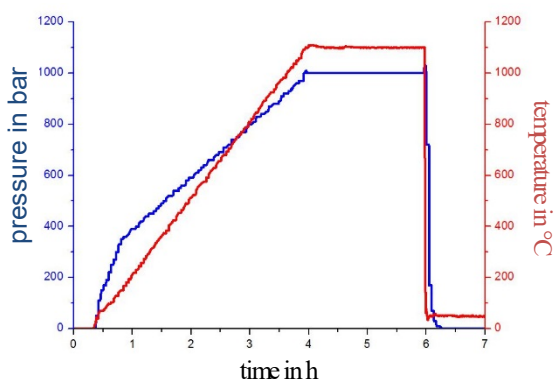

Fig. 2. Temperature and pressure profile of the HIP profile

For the thermal treatment of solution annealing we use the same parameters as for HIP cycle. Accordingly a heating rate of $\Delta\vartheta_{heat}$ = 5 K/min, reaching a temperature of ϑ_{max} = 1100°C with a holding time of t_{hold} = 2 h.

The high cooling rate is approximated by water-quenching. For the hot isostatic pressing we use the system QIH 15L, Quintus Technologies and for solution annealing we use the furnace LH 120/12, Nabertherm.

The tensile test of the specimens relates to DIN EN ISO 7438 using the system AG-X plus, Shimadzu Europa GmbH. The constant traverse speed is set to $v_{traverse}$ = 1 mm/min. For determination of the porosity of the specimens and the metallographic inspection we use micrographic analysis. The preparation of the specimens is done by polishing with diamond suspension down to a granularity of g_{dsus} = 1 µm and surface etching (Adler formulation) Petzow, 2015.

3. Results

We start our analysis by verifying the densification of the specimens by applying the HIP cycle shown in Figure 2. The relative densities are estimated by microscopic inspection of the layers shown in Fig. 3. The black areas indicate pores. The densification process by hot isostatic pressing can clearly be observed by comparing the AB (Fig. 3, above) with HIP (Fig.3, below) specimens. For the AB specimens we measure a relative density of ρ_{rel} = 97,30 % and for the HIP specimens a relative density of ρ_{rel} = 99,90 %. Accordingly the HIP cycle has led to a reduction of the porosity of $\Delta\rho_{rel}$ = 2,6 %.

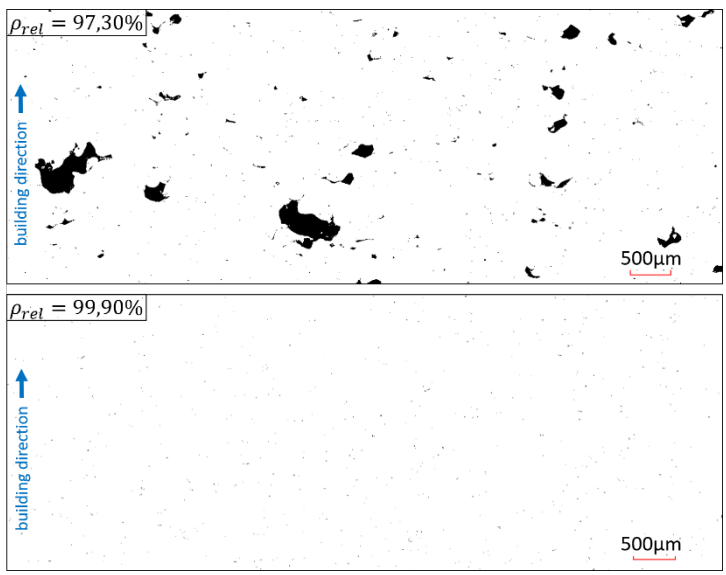

Fig. 3. Microscopic identification of porosity of as-buid (above) and HIP (below) specimens

We fabricate tensile test specimens in five different orientations regarding the building plate and measure tensile strengths and failure strains. The results for the AB specimens are shown in Fig. 4 (blue). The dependency of the building direction is obvious and agrees with literature values in Mooney, 2019 and Bräunig, 2015 (Figure 4a, gray, green). The directional dependency may result through an increase of the influence of lack-of-fusion porosity with increasing orientation angle. The decrease of the failure strain at the same time supports this assumption Hardin, 2016.

The scattering of values of the tensile strength in each building orientation may result through variation of porosity and pore morphologies of the specimens. The local increase of the tensile strength around the building orientation of 45° can not be confirmed by literature values (see Fig. 4a). But considering literature values of stainless steel a similar characteristic can be found on the basis of molybdenum segregations at the grain boundaries Shifeng, 2014; Wawoczny, 2018; Buchanan, 2017; Qiu, 2018. The studied 1.2709 steel consists of a significant percentage of molybdenum (see Tab. 1) that could explain the local increase of the tensile strength.

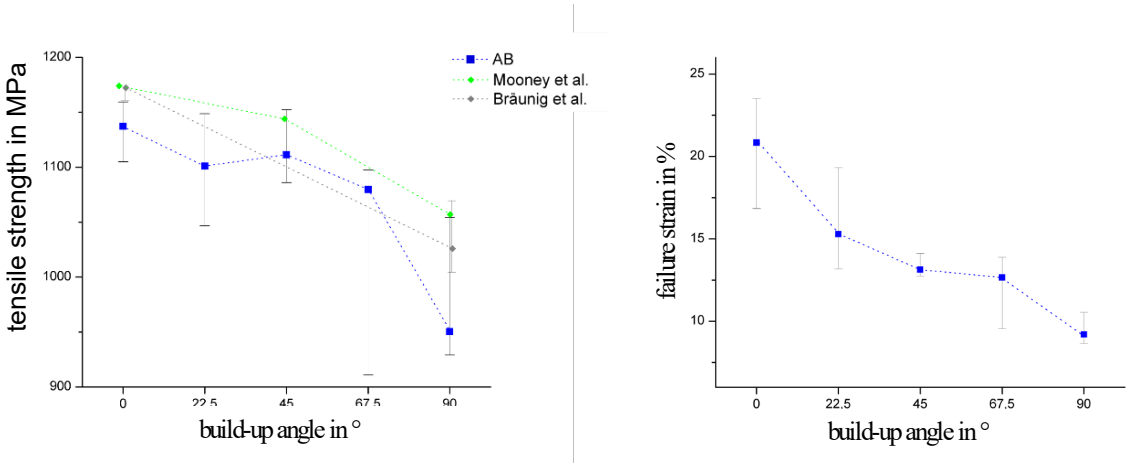

Fig. 4. a) Tensile strength and b) failure strain regarding the build-up orientation

Next we apply the thermal treatments of solution annealing and hot isostatic pressing. In Figure 5 the metallographic inspection of as-build, solution annealed and hot isostatic pressed specimens is shown.

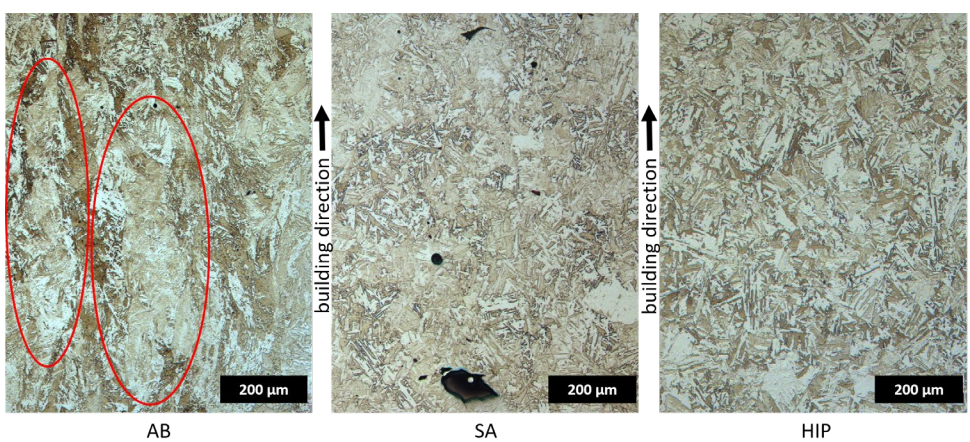

AB SA HIP

Fig. 5. Microstructure of as-build (AB), solution annealed (LG) and hot isostatic pressed (HIP) specimens

In the microstructure of AB specimens a directional grain structure in building direction can be observed. In the microstructure of SA and HIP specimens a directional grain structure is not clearly visible. Here the randomly distributed martensitic needles mask the grain structure. This indicates a rearrangement of the structural conditions by solution annealing and hot isostatic pressing. Considering the solution annealed specimens lack-of-fusion pores as well as gas pores can be found. By comparing the porosity of the SA and HIP specimens a significant reduction of the porosity in the HIP condition can be observed.

The measurements of the tensile strength of SA and HIP specimens and combined with the AB specimens are shown in Fig. 6.

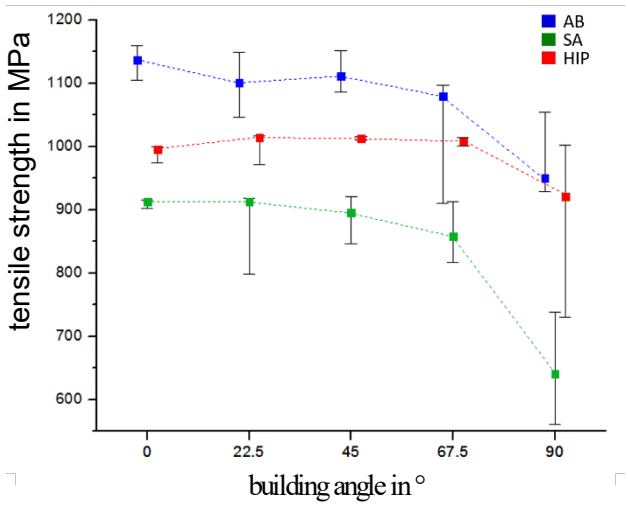

Fig. 6. Tensile strength of as-build (AB), solution annealed (LG) and hot isostatic pressed (HIP) specimens

Comparing the results of AB (blue) and SA (green) two features can be found. Firstly the local increase of the tensile strength around the building orientation of 45° has disappeared. This may be caused by a rearrangement of the structural conditions. Additionally the lower cooling rates in solution annealing compared to the SLM process enhance the solubility of molybdenum accordingly a lower segregation occurs. Secondly the tensile strength of the SA specimens is significantly reduced. The reason may found by closer inspection of the microstructure. In Fig. 7 a higher resolution of the microstructure of AB, SA an HIP specimens is shown.

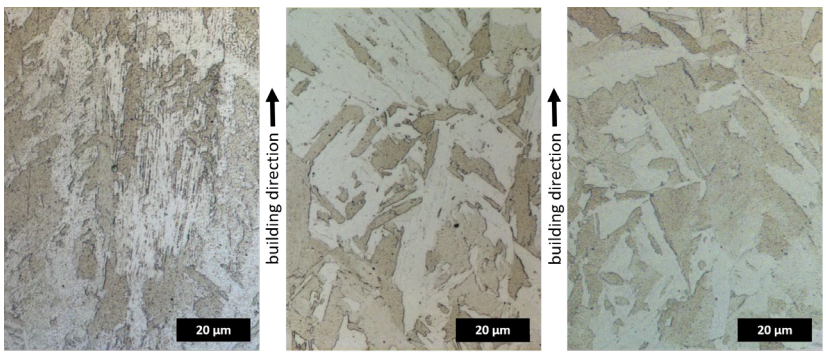

Fig. 7. Submicrostructrue of as-build (AB), solution annealed (SA) and hot isostatic pressed (HIP) specimens

In the microstructure of the AB specimens a fine grain substructure appears which may be caused by high cooling rates in SLM fabrication. This substructure is related to high dislocation densities which leads to higher values of the tensile strength. As shown in Fig. 7 the substructure disappears by applying the SA or HIP process and martensite blocks (white) are formed. This results from the reduction of dislocations by diffusion Becker, 2016; Casati 2016; Bürgel, 2011.

Comparing the tensile strength of AB and LG specimens with the values of the HIP specimens three features can be found. Firstly the values of the tensile strength is between the values of the AB and LG specimens. Secondly the local increase of the tensile strength disappears also in the HIP process. Thirdly the directional dependency of the tensile strength is significantly reduced. The drop of the values for building orientation of 90° may result from outliners. These specimens showed oxidization on the fracture surface which indicates surface connected porosity that could not be closed through HIP treatment and may have led to early failure. Regarding the thermal profile hot isostatic pressing is comparable to solution annealing. By comparing the results of the HIP specimens to the SA specimens the local increased tensile strength around 45° also disappears and the global tensile strength is also reduced compared to the AB condition. As mentioned this results by dissolving of the grain substructure and by rearrangement of the structural conditions. Accordingly the higher values of HIP compared to SA, the reduction of the directional properties and as well as the reduction of the scattering can be derived from the reduction of the porosity using HIP treatment. These results are in agreement with fractographical analysis in Masneri, 2016 were the porosity in the volume was identified as one of the main reasons for early failures of 1.2709 specimens.

4. Conclusion

We analyzed the effects of solution annealing and hot isostatic pressing on SLM fabricated specimens using maraging tool steel 1.2709.

A fine-grained substructure was found for as-build specimens. This substructure induces high values of tensile strength. By solution annealing and hot isostatic pressing the substructure disappears and the tensile strength decreases. The dominating effect of the directional mechanical properties results mainly from lack-of-fusion porosity in the volume. By applying hot isostatic pressing the porosity can be reduced which leads

to a nearly isotropic characteristic of the tensile strength. Furthermore the scattering of values can be significantly reduced. Even though the densification leads to a higher tensile strength compared to SA condition. But due to the high temperatures in the HIP-process the fine-grained substructure disappears and reduce the global strength of the material compared to the AB condition.

In further studies we want to evaluate how the porosity can be reduced by preserving the substructure. In addition the influence of the morphology of the pores regarding directional mechanical properties should be examined.

References

Gibson, L., Rosen, D., Stucker, B., 2015. Additive Manufacturing Technologies 2nd Edition. Springer Verlag, New York.

Yap, C., Chua, C., Dong, Z., Lui, Z., Zhang, D., Loh, L., Sing, L., 2015. Review of selective laser melting: material and applicatios. Applied Physics Reviews 041101, p. 1.

Seabra, M., Azevedo, J., Araújo, A., Reis, L., Pinto, E., Alves, N., Mortágua, J., 2016. Selective Laser Melting (SLM) and topology optimization for lighter aerospace components. Procedia Structural Integrity 1, p. 289.

Colter, B., Small, G., 2017. Linear AMS: How an AM service provider is embracing the new infrastructure of on demand manufacturing. Metal Additive Manufacturing 3, p. 78.

Ilschner, B., Singer, R. F., 2010. Werkstoffwissenschaften und Fertigungstechnik (Springer-Lehrbuch). Springer Verlag Berlin, Heidelberg.

Niendorf, T., Leuders, S., Riemer, A., Richard, H. A., Tröster, T., Schwarze, D., 2013. Highly Anisotropic Steel Processed by Selective Laser Melting, Metallurgical and Materials Transactions B 44, 4, p. 794.

Buchmayr, B., Panzl, G., Walzl, A., Wallis, C., 2017. Laser Powder Bed Fusion - Materials Issues and Optimized Processing Parameters for Tool steels, AlSiMg- and CuCrZr-Alloys, Advanced Engineering Materials,19, p. 1600667.

Kruth, J.-P., Badrossamay, M., Yasa, E., Deckers, J., Thijs, L., van Humbeeck, J., 2010. Part and material properties in selective laser melting of metals, Proceedings of the 16th International Symposium on Electromachining, 16, p. 1.

Mercelis, P., Kruth, J.-P., 2016. Residual stresses in selective laser sintering and selective laser melting, Rapid Prototyping Journal, 12, p. 254.

Rösler, J., Bäker, M., Harders, H., 2016. Mechanisches Verhalten der Werkstoffe: Mit 31 Tabellen und 34 Aufgaben und Lösungen. 2., durchges. und erw. Aufl. Teubner Verlag, Wiesbaden.

Kempen, K., Yasa, E., Thijs, L., Kruth, J.-P., van Humbeeck, J., 2011. Microstructure and mechanical properties of Selective Laser Melted 18Ni-300 steel, Physics Pro-cedia, 12, p. 255.

Cáceres, C. H., Selling, B. I., 1996. Casting defects and the tensile properties of an AlSiMg alloy, Materials Science and Engineering: A 220, p. 109.

Cherry, J. A., Davies, H. M., Mehmood, S., Lavery, N. P., Brown, S. G. R., Sienz, J., 2015. Investigation into the effect of process parameters on microstructural and physi-cal properties of 316L stainless steel parts by selective laser melting, International Journal of Advanced Manufacturing Technology, 76, p. 869.

Ganeriwala, R., Zohdi, T. I., 2016. A coupled discrete element-finite difference model of selective laser sintering, Granular Matter, 18.

Wessels, H., Gieseke, M., Weißenfels, C., Kaierle, S., 2017. Simulation von Selective Laser Melting Prozessen, In: Lachmayer, R. (Hrsg.): Additive Manufacturing Quantifiziert: Visionäre Anwendungen und Stand der Technik. Springer Vieweg, Berlin, Heidelberg, p. 145.

Karg, M., 2012. Laserstrahlschmelzen von Metallen – aktuelle Entwicklungen im Bereich der Additiven Fertigung. In: Schmidt, M.; Roth, S.; Amend, P. (Hrsg.): Tagungsband: LEF 2012, Meisenbach Verlag, Bamberg, p. 223.

Khairallah, S. A., Anderson, A. T., 2014. Mesoscopic Simulation Model of Selective Laser Melting of Stainless Steel Powder, Journal of Materials Processing Technology, 214, p. 2627.

Zhang, B., Ham, K., Shao, S., Shamsaei, N., Tompson, S. M., 2017. Effect of Heat Treat-ment and Hot Isostatic Pressing on the Morphology and Size of Pores in Additive Manufactured Ti-6Al-4V Parts, Solid Freeform Fabrication 2017: Proceedings of the 28th Annual International Solid Freeform Fabrication Symposium – An Additive Manufacturing Conference, p. 107.

Wycisk, E., 2017. Ermüdungseigenschaften der laseradditiv gefertigten Titanlegierung TiAl6V4. Springer Verlag, Berlin, Heidelberg.

Du, W., Bai, Q., Zhang, B., 2016. A novel method for additive/subtractive hybrid manufacturing of metallic parts. Procedia Manufacturing 5, p. 2018.

Atkinson, H. V.; Davies, S., 2000. Fundamental aspects of hot isostatic pressing: An overview, Metallurgical and Materials Transactions A, 31, p. 2981.

Petzow, G., 2015. Metallographisches, keramographisches, plastographisches Ätzen. 7. leicht korrigierte Auflage (Materialkundlich-technische Reihe 1), Gebrüder Borntraeger, Stuttgart.

Mooney, B., Kourousis, K. I., Raghavendra, R., 2019. Plastic anisotropy of additively ma-nufactured maraging steel: Influence of the build orientation and heat treatments, Additive Manufacturing, 25, p. 19.

Bräunig, J., Töppel, T., Müller, B., Burkhardt, M., Hipke, T., Drossel, W.-G., 2015. Advanced Material Studies for Additive Manufacturing in terms of Future Gear Ap-plication, Advances in Mechanical Engineering, 6, p. 741083.

Hardin, R. A., Beckermann, C., 2016. Effect of Cooling Rate and Microporosity on Mechanical Performance of a High Strength Steel, Proceedings of the 70th SFSA Technical and Operating Conference, 5.2.

Shifeng, W., Shuai, L., Qingsong, W., Yan, C., Sheng, Z., Yusheng, S., 2014. Effect of molten pool boundaries on the mechanical properties of selective laser melting parts, Journal of Materials Processing Technology, 214, p. 2660.

Wawoczny, D., Weber, S., Schneider, M., 2018. Statische Festigkeit eines additiv gefertigten 316L nach dem Lösungsglühen, Prozesswärme, p. 59.

Buchanan, C., Matilainen, V.-P., Salminen, A., Gardner, L., 2017. Structural performance of additive manufactured metallic material and cross-sections, Journal of Constructional Steel Research, 136, p. 35.

Qiu, C., Kindi, M. A., Aladawi, A. S., Hatmi, I. A, 2018. A comprehensive study on microstructure and tensile behaviour of a selectively laser melted stainless steel, Scientific reports, 8, p. 7785.

Becker, T. H., Dimitrov, D., 2016. The achievable mechanical properties of SLM pro-duced Maraging Steel 300 components, Rapid Prototyping Journal, 22, p. 487.

Casati, R., Lemke, J., Tuissi, A., Vedani, M., 2016. Aging Behaviour and Mechanical Performance of 18-Ni 300 Steel Processed by Selective Laser Melting, metals 6, p. 216.

Bürgel, R., Jürgen Maier, H., Niendorf, T.: Handbuch Hochtemperatur- Werkstofftechnik: Grundlagen, Werkstoffbeanspruchungen, Hochtemperaturlegierungen und -beschichtungen; mit 66 Tab. 4., überarbeitete Auflage (Praxis), Vieweg Teubner Verlag, Wiesbaden.

Masneri, C., 2016. Microstructural and mechanical properties of maraging steel parts produced by selective laser melting.